Journal of Ceramic Processing Research. Vol. 14, No. 1, pp. 139~143 (2013)

J O U R N A L O F
Ceramic Processing Research

The influence of processing parameters on structural and luminescent characteristics of an Eu^{2+}-doped Sr-Si-O-N system

Dong Wook Suh, Gopinathan Anoop, In Hyun Cho, Jae Soo Yoo, Soo Young Kim and See Hee Shin*

School of Chemical Engineering and Materials Science, Chung-Ang University, 221, Heukseok-Dong, Dongjak-gu, Seoul 156-756, Korea

Eu^{2+}-doped Sr-Si-O-N material phosphors were synthesized using a high temperature solid state reaction. High solubility of nitrogen in an oxynitride system is known as a labored process when it occurs under high nitrogen pressure. The factors influencing structural and luminescent characteristics of Eu^{2+}-doped $SrSi_2O_2N_2$ system have been investigated in detail. In a $SrSi_2O_2N_2$ system, the peak emission spectra change with processing parameters such as gas flow rate, which results in a different O/N ratio. The optical and structural properties are also dependent upon the reaction temperature and reaction period. For instance, the $SrSi_2O_2N_2:Eu^{2+}$ system is converted into a $Sr_2Si_5N_{8-\alpha}O_\alpha$ system when exposed to a longer reaction at higher temperature. XPS and FTIR analyses confirm the variation in structural changes which affect the emission wavelength of the phosphor. This metamorphosis seems to be related to the unstable longevity of oxynitride material phosphors.

Key words: Oxynitride, Phosphor, LED, Spectrum.

Introduction

Solid state lighting devices are alternatives for conventional light sources such as incandescent and fluorescent lamps. The advantages of solid-state lighting devices based on pc-LED are a longer lifetime, lower energy consumption, and higher efficiency than conventional lamps. $(Y_{1-a},Gd_a)_3(Al_{1-b},Ga_b)_5O_{12}:Ce^{3+}$(YAG:$Ce^{3+}$) [1, 2], $Sr_2SiO_4:Eu^{2+}$ [3], and $Eu_{0.00296}Si_{0.41395}Al_{0.01334}O_{0.0044}N_{0.56528}$ (β-SiAlON) [4] have been commercialized for phosphor conversion based on InGaN LED blue chips. White light is generated by a combination of blue light from the InGaN-based LED chip and yellow light from YAG, which has a poor color rendering index and thermal quenching at high temperature [5]. White light-emitting devices are also fabricated using green and red phosphors excited by a blue LED (Sr_2SiO_4 or β-SiAlON and $CaAlSiN_3$ excited by blue light) [1-6].

The $SrSi_2O_2N_2$ system has been studied since it was reported by Zhu in 1994 [7]. Li. et al. [8] found it to be monoclinic, while the structures of both $SrSi_2O_2N_2$ and $EuSi_2O_2N_2$ were found to be triclinic by Oeckler, who utilized a Le Bail fit of an X-ray powder pattern [9]. In recent years, $SrSi_2O_2N_2:Eu^{2+}$ has been found to be a promising green-phosphor for white LEDs due to its excellent thermal resistance, high efficiency, and chemical stability [10]. Therefore, oxynitride phosphor is undergoing study with several analytic methods. Schnick et al. reported the crystal structures of single crystals of $M_2Si_5N_8$ (M = Sr, Ba, Ca) that, for Sr and Ba, form an orthorhombic lattice with the space group $Pmn2_1$ [11] and a monoclinic crystal with the space group of *Cc* for Ca [12]. Many studies have been conducted to show that silicon-based nitride composites have good crystal and optical properties compared with red luminescent materials [13, 14]. However, silicon-based nitride composites are not yet used for commercialized white LEDs to our knowledge.

Yun et el. [10] reported XRD patterns of $SrSi_2O_2N_2:Eu^{2+}$ with varying firing temperatures up to 1400 °C. The crystal structure of $SrSi_2O_2N_2:Eu^{2+}$ forms under the influence of high firing temperatures. Li [14] and Xie et al. [15] demonstrated that red-emitting phosphors could be synthesized under various processing parameters, which can make solid-state lighting very easy and reasonable. Anoop et al. [16] readily synthesized $Sr_2Si_5N_8$ from a $Sr_2Si_3O_2N_4$ composition. However, the parameters that influence phase transition and optical properties have not been known ever such as reducing gas volumetric flow rate, calcinations temperature and firing time.

In this work, we study the effects of processing parameters on phosphor synthesis, particularly, the structural and luminescent characteristics of a typical oxynitride $SrSi_2O_2N_2:Eu^{2+}$ phosphor. The optical and structural variations of the Sr-Si-O-N system at various conditions of gas flow rate and temperature are discussed. It is interesting to note that even though initial molar ratios of constituent chemicals such as $SrCO_3$ and Si_3N_4 are kept constant, varying the gas flow rate, reaction time and temperature may end up in different phosphor systems.

*Corresponding author:
Tel :
Fax:
E-mail: shshin@cau.ac.kr

Experimental

Phosphor samples were synthesized using a conventional solid-state reaction at a relatively low firing temperature. The main starting materials for the $SrSi_2O_2N_2$ phosphors were $SrCO_3$ (99.9%, Kojundo), Eu_2O_3 (99.99%, Kojundo), and Si_3N_4 (99.9%, Ube industries). The starting materials were mixed at molar ratios with the desired stoichiometric ratio and ball-milled with acetone. The mixtures put into carbon crucibles were heated at 1200-1500 °C for 6 hr/12 hr at volumetric flow rates in the range of 300 - 500 cc/min in a reducing atmosphere (H_2:N_2 = 5%:95%) using a tube furnace. The reducing gas flow rates were controlled using mass flow controller. The Eu^{2+} concentration was fixed at 0.07 mol% throughout the study.

The synthesized phosphors were characterized by an X-ray diffractometer (XRD; Bruker, New D8-Advance-AXS, 40 kV and 40 mA) using Cu Kα radiation. The room temperature photoluminescent emission (PL) and excitation (PLE) spectra were recorded using a PMT and Xenon lamp (PSI, Korea). X-ray Photoelectron Spectroscopy (XPS) spectra were recorded using a Thermo Scientific, K-α with a monochromated Al Kα anode. IR measurements were carried out using a Fourier transform infrared Nicolet 6700 Spectrometer (Thermoscientific, U.S.A) with KBr as a reference. The oxygen and nitrogen levels were examined by an oxygen/nitrogen analyzer (TC-600, LECO Co.)

Results and Discussion

Fig. 1(a) shows XRD patterns of the phosphor synthesized at various gas flow rates. From Fig. 1(a), it is clear that the dominant phase is $SrSi_2O_2N_2$:Eu^{2+} (PDF #01-076-3141). Even if the samples synthesized at 300 and 400 cc/min have a nearly single phase of $SrSi_2O_2N_2$:Eu^{2+}, traces of strontium silicon nitride ($Sr_2Si_5N_8$, PDF #01-085-0101) phase appear for that synthesized at 500 cc/min. We suspect that high volumetric gas flow rates promote substitution of nitrogen into the $SrSi_2O_2N_2$ lattice, together with a carbothermal reaction, as reported by Piao et.al, due to the use of carbon crucibles [17]. Fig. 1(b) shows that the phosphor synthesized at 1350 °C and reducing gas flow rate (500cc/min) for 6hr has a nearly single phase of $SrSi_2O_2N_2$, while that synthesized at 1400 °C for the same period has a dominant $SrSi_2O_2N_2$ phase and traces of $Sr_2Si_5N_8$. A possible reaction route may be as following ;

$$3SrCO_3 + 1.5SiO_2 + 1.5Si_3N_4 \rightarrow xSr_2Si_5N_8 + ySrSi_7N_{10} \quad @\ 1500\ ^\circ C,\ 500\ cc/min\ and\ 12\ hr \qquad (1)$$

However, the phosphor synthesized at 1500 °C crystallizes in $Sr_2Si_5N_8$ structure along with traces of the $SrSi_2O_2N_2$ phase. All the phosphors were synthesized in a tubular reactor so that both the $SrSi_2O_2N_2$:Eu^{2+} phase and the oxygen-contaminated strontium silicon nitride phase ($Sr_2Si_5N_8$) are obtained at 1500 °C (6 hr and 500 cc/min). In order to analyze the effect of reaction time, phosphors were also synthesized at various calcination times. It is believed that sufficient calcination/reaction time could result in a single-phase phosphor. The phosphor synthesized at 1500 °C and reducing gas flow 500 cc/min for 12 hrs crystallizes in $Sr_2Si_5N_8$ with traces of $SrSi_7N_{10}$. This is quite natural since initial molar ratios are not chosen to get an end product $Sr_2Si_5N_8$. However, the oxygen impurities in the samples could not be explained from XRD patterns and are discussed later. From the XRD results, it is clear that a nearly single phase $SrSi_2O_2N_2$ structure is obtained only when the phosphor is synthesized at 1350 °C (300 cc/min and 6 hr). It should be noted that, among processing parameters, calcination temperatures and firing times are important to obtain strontium silicon nitride phase from these results.

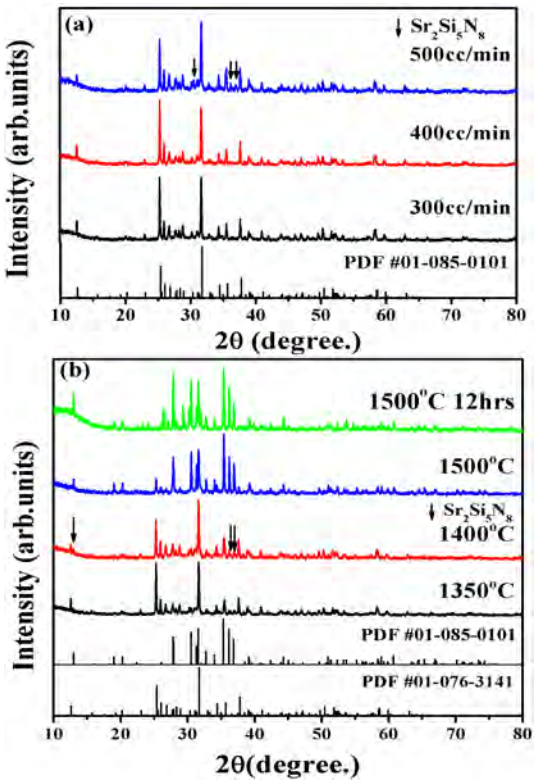

Fig. 1. XRD patterns of $SrSi_2O_2N_2$:Eu^{2+} phosphors at various (a) flow rates of reducing gas fixing 1350 °C and reaction period (6hr) and (b) firing temperatures fixing flow rates (500 cc/min) of reducing gas and reaction period (6 hr).

Fig. 2(a) shows the PL emission spectrum for $SrSi_2O_2N_2$:Eu^{2+} as synthesized at various flow rates (300 - 500 cc/min) at 1350 °C for 6 hrs. The emission can be attributed to the $4f^6\ 5d \rightarrow 4f^7$ transition in the Eu^{2+} ion [14]. The PL peak emission wavelength experiences a slight red shift with a resulting increase in the flow rate of ambient gas, which could be due to the increased nitrogen incorporated into the lattice at

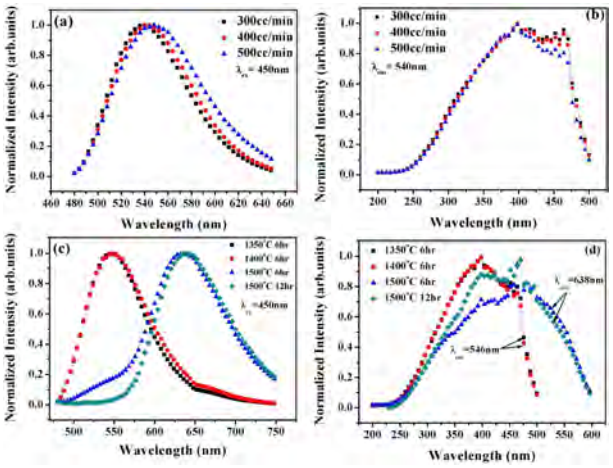

Fig. 2. (a) PL emission and (b) PLE spectra of the $SrSi_2O_2N_2:Eu^{2+}$ phosphor at various reducing gas flow rates fixing firing temperature (1350 °C) and reaction period (6 hr), (c) PL emission and (d) PLE spectra of the $SrSi_2O_2N_2:Eu^{2+}$ phosphor at various reaction temperatures and times fixing flow rates of reducing gas (500 cc/min).

Table 1. O/N ratio of the $SrSi_2O_2N_2:Eu^{2+}$ phosphor for various gas flow rates, reaction temperatures, and times.

Condition	O at%	N at%
1350 °C 6 hrs 300 cc/min	49.32	50.68
1350 °C 6 hrs 500 cc/min	41.28	58.72
1500 °C 12 hrs 500 cc/min	3.77	96.23

higher flow rates. Fig. 2(b) shows the PLE spectrum for $SrSi_2O_2N_2:Eu^{2+}$ synthesized at various flow rates at 1350 °C for 6 hrs. The spectrum has a broad region from 270 to 460 nm which can be attributed to the crystal-field components at the 5d level in the excited $4f^65d^1$ configuration of the Eu^{2+} [10]. The PL emission spectra of the phosphors synthesized at various calcination temperatures are shown in Fig. 2(c). It is quite evident from the figure that, as the calcination temperature is increased to 1500 °C, the peak emission wavelength shifts to 625 nm. From the XRD analysis, it is apparent that the crystal structure of the phosphor synthesized at 1500 °C (6 hr and 500 cc/min) is of $Sr_2Si_5N_8$ structure. This variation in crystal structure resulted in a considerable red shift in the PL spectra. The O/N ratio of the as-synthesized phosphors is shown in Table 1. When varying gas flow rates, the content of nitrogen increases with increase in gas flow rate 500 cc/min in which the pressure of the reducing gas is raised slightly under the same temperature. Such a rising pressure may result in a little high partial pressure of nitrogen gas in the reactor, thus helping incorporating into the lattice. The PL and PLE spectra with varying temperatures and times are shown in Fig. 2(c) and (d), respectively. Both figures have typical characteristics for each material system. The PL and PLE of 1350 °C and 1400 °C also have properties that were mentioned in a previous section. However, the

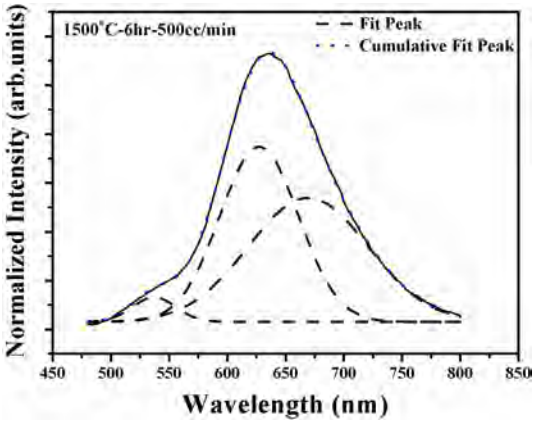

Fig. 3. Deconvoluted-PL emission spectra at 1500 °C for 6 hrs at 500 cc/min.

cases of 6 hr and 500 cc/min and 12 hr and 500 cc/min at 1500 °C take on new significance. Since the former is the phosphor crystallized in the $Sr_2Si_5N_8$ structure along with traces of the $SrSi_2O_2N_2$ phase, it has some properties of $SrSi_2O_2N_2$, such as a 540 nm peak emission wavelength and a higher intensity excitation peak than at 1500 °C (12 hr and 500 cc/min). Based on the phase transition for reaction times from 6 hr to 12 hr at 1500 °C, the properties of each material system also revert to their original states. Consequently, at 1500 °C (12 hr, 500 cc/min), the emission peak of $SrSi_2O_2N_2$ disappears. In addition, the emission wavelength was found to be 610 - 640 nm for Eu $(Sr2)^{2+}$ and 655 - 670 nm for Eu $(Sr1)^{2+}$, similar to that of previous reports [14-16]. The crystal structure of the phosphor is similar to that of the $Sr_2Si_5N_8$ system, possibly due to two Sr sites with coordination numbers of 8 (Sr1) and 10 (Sr2) [17]. Hence, the PL emission in the short wavelength region (610 - 640 nm) may be attributed to emission from Eu$(Sr2)^{2+}$. On the other hand, the emission from the longer wavelength (655 - 670 nm) is from Eu $(Sr1)^{2+}$ [16]. The photoluminescent excitation spectra of the phosphor synthesized at 1500 °C for 12 hrs are composed of broad band spreading from 250 to 500 nm.

The PL emission of the phosphor synthesized at 1500 °C can be roughly deconvoluted into three peaks and is shown in Fig. 3. Since the crystal phase at 1500 °C (6 hr and 500 cc/min) is mixed with $SrSi_2O_2N_2$ and $Sr_2Si_5N_8$ phases, the PL spectrum is shown as a combination of peaks at 537 nm for $SrSi_2O_2N_2$ and 627 and 669 nm for the $Sr_2Si_5N_8$ phase. The emission spectrum for excitation at 450 nm shows a broad band peak at 635 nm, which is ascribed to the allowed $4f^6$ 5d $\rightarrow 4f^7$ transition of Eu^{2+} ions. The emission of the $Sr_2Si_5N_8:Eu^{2+}$ phosphor appears at a much longer wavelength compared with that of $Sr_2SiO_4:Eu^{2+}$. This may be ascribed to the higher electronegativity and nephelauxetic effect of the N^{3-} ion [17].

In the cases of $Sr_2Si_5N_8:Eu^{2+}$ and $Ba_2Si_5N_8:Eu^{2+}$, the emission band of Eu^{2+} subsequently shifts from orange

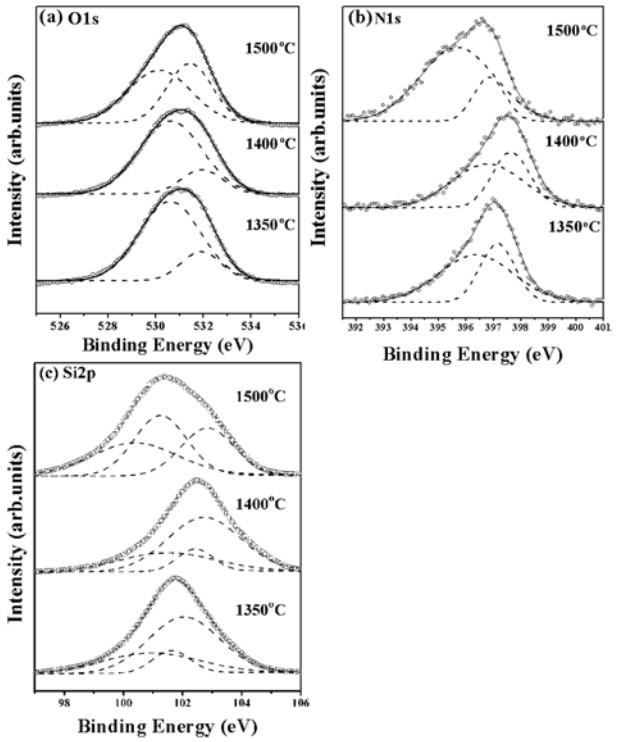

Fig. 4. XPS spectra of the (a) O 1s region, (b) N 1s, and (c) Si 2p in $SrSi_2O_2N_2:Eu^{2+}$ phosphor for various reaction temperatures fixing flow rates of reducing gas (500 cc/min) and reaction period (6 hr).

for Sr and yellow for Ba at low Eu^{2+} concentrations into the red region for high Eu^{2+} concentrations up to 680 nm. $Sr_2Si_5N_8$ has two crystallographic Sr sites. The presence of only a single broad emission band suggests that the environment of both Eu^{2+} ions is not very sensitive to changes in the local structure, eventually resulting in large overlap between the two emission bands of Eu^{2+} [14]. However, Fig. 3 does not show the presence of a single emission spectra, indicating that $Eu(Sr2)^{2+}$ and $Eu(Sr1)^{2+}$ ions experience different crystal field strengths and that they are sensitive to changes in the local structure. At 1500 °C (6 hr and 500 cc/min), it has the structure of $Sr_2Si_5N_8$ with oxygen added. It is necessary to show why the emission peak of the sample is different from those of pure $Sr_2Si_5N_8$:Eu and $SrSi_2O_2N_2$:Eu.

To find variation in the emission wavelength from $Sr_2Si_5N_8$ and the existance of oxygen in the lattice, an XPS study was carried out. Fig. 4 shows the high resolution XPS spectrum of O 1s, N 1s and Si 2p for phosphor synthesized at 1350 °C, 1400 °C, and 1500 °C under 500 cc/min for 6 hr. We express the notation of individual samples as 1350 °C, 1400 °C, and 1500 °C since they were obtained under the same conditions; reducing gas flow rate (500 cc/min) and reaction period (6 hr). As shown in the XPS results of the powder samples, O 1s, N 1s and Si 2p peaks are broad and not symmetric. They were roughly deconvoluted into two peaks. Scattered circles and solid lines represent the raw data, and dashed lines are the fitted data. The binding energy of O 1s in SiO is 532.5 eV [18] and one of the fitted-peaks of the 1350 °C and 1400 °C samples is observed at (531.9 eV) as shown in Fig. 4(a) which is slightly shifted to lower binding energy. This indicates that the samples has Si-O-Sr bondings in the structure of $SrSi_2O_2N_2$. With increased firing temperature to 1400 °C, the binding energy peak shift doesn't occur. With that structure, if the incorporation of oxygen decreases, its intensity spontaneously can be reduced. The binding energy of O 1s in SrO is reported to be 530.2 eV [19]. Crystal bonding of Sr-O-Sr can exist in $SrSi_2O_2N_2$ in which the electron density of oxygen decreases due to the bonding. As a result, the binding energy values at 1350 °C and 1400 °C lies in the higher region, 530.6 eV. On the other hand, the sample at 1500 °C contains $Sr_2Si_5N_{5-a}O_a$ and some $SrSi_2O_2N_2$, as shown in Fig. 2, and has a small emission peak at 540 nm. Decreasing the amount of oxygen incorporated into SiO_xN_y shifts the binding energy of O 1s to lower region (531.4 eV) and its intensity indicates also increasing due to the nitridation of the phosphor as a silicon nitride phosphor phase at higher temperature (1500 °C) compared with those of Si-O-Sr, which has a binding energy of 530.2 eV. Therefore it suggests that the phosphor synthesized at 1500 °C contains the small oxygen contents and it can consist of $Sr_2Si_5N_{5-a}O_a$ to produce variation in the PL emission wavelength. The XPS binding energy spectrum of N 1s is similar to the O 1s spectrum, as shown in Fig. 4(b). As the both binding energy values of O 1s at 1350 °C and 1400 °C are same, those of the N 1s do not mean a significant discrepancy, producing values of 397.2 [20] and 397.6 eV, respectively. At 1500 °C, the binding energy of 396.9 eV is from SiO_xN_y and is of a lower intensity than that of the sample that contains relatively high oxygen contents and has a binding energy of 395.7 eV. We estimate that 395.7 eV is the binding energy of Sr-N-Si. Fig. 4c shows the Si 2p high resolution XPS binding energy value of phosphor samples synthesized at various temperature under the same gas flow rate and reaction period (500 cc/min and 6 hr). With the change of reaction temperautre, the binding energy value (102.0 eV) move to higher (102.7 eV), which is originated from SiO_xN_y. 100.9 and 101.6 eV from SiO_x at 1350 °C varies shift to 101.5 and 102.4 eV, repectrively. At 1500 °C 100.4 and 101.3 may be originated from Si and 102.9 eV also from SiO_xN_y. It indicates that the phosphor samples have undergone nitridation with varying reaction temperature. Especially it means that the sample obtained at 1500 °C contains both Si-N and oxygen incoportated into Si-N structure. From the oxygen levels in Table 1, dissolution of oxygen in the lattice is concluded to reduce covalency between Si and N. However, the change in the PL spectrum is not significant due to the binding energy shift. The case of sample synthesized at 1500 °C for 12 hr is different from the previous one due to structural differences.

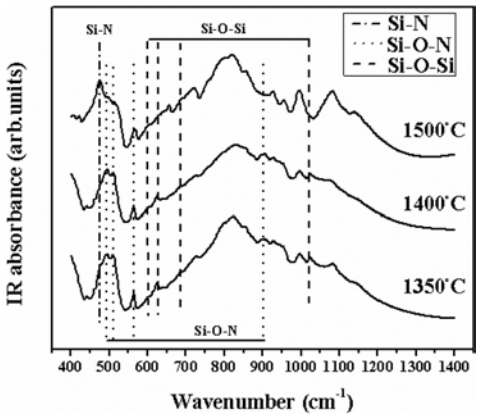

Fig. 5. IR absorption spectra of the $SrSi_2O_2N_2:Eu^{2+}$ phosphor for various reaction temperatures fixing flow rates of reducing gas (500 cc/min) and reaction period (6 hr).

Fig. 5 shows the FTIR spectra of samples synthesized at 1350 ºC, 1400 ºC, and 1500 ºC. The spectra at 1350 ºC and 1400 ºC are consistent, as shown in Fig. 5. The bands located at about 600 - 700 cm^{-1} and 1025 cm^{-1} are attributed to the Si-O-Si vibration mode. The vibration of Si-N at 460 cm^{-1} and vibrations of Si-O-N around 490 - 565 cm^{-1} and 900 cm^{-1} were observed [21]. Although vibration peaks of 1350 ºC, 1400 ºC, and 1500 ºC are similar at 900 cm^{-1} (Si-O-N) and at the first peak around 563 cm^{-1}, solid peaks at 490 - 565 cm^{-1} exist only at 1350 ºC and 1400 ºC. After an increase in the peak of Si-N around 474 cm^{-1}, the subsequent two peaks of Si-O-N may be weak. The existence of the Si-N bond indicates a red-emitting phosphor. $Sr_2Si_5O_xN_8$ containing oxygen, and Si-O and Si-N stretching vibrational absorptions are in the 800 - 830 cm^{-1} range [22]. All the samples have maximum absorbance at 800 - 830 cm^{-1}, indicating the Si-O and Si-N stretching vibration mode. The 1500 ºC sample also contains oxygen in $Sr_2Si_5N_8$ and in a small portion of $SrSi_2O_2N_2$.

Conclusion

The structural and luminescent characteristics of Eu^{2+}-doped Sr-Si-O-N material system phosphors were studied by varying firing temperature and gas flow rate. We observed that structure changes occur during the transition from the dominant $SrSi_2O_2N_2$ phase to $Sr_2Si_5O_xN_x$ at various temperatures. The PL emission peak experiences slight red shifts with increasing flow rate for phophors synthesized at 1350 ºC, ascribed to increased nitrogen content. When varying reaction temperatures with excess gas flow, the emission peak shift no longer occurs. Instead, the $SrSi_2O_2N_2$ structure is transformed into a new structure, $Sr_2Si_5N_8$. However, these are not pure crystal structures such as that of $Sr_2Si_5N_8$ and are obviously contaminated by oxygen. XPS and FTIR analyses provide information on local structure variation which affects the PL emission characteristics in the Sr-Si-O-N system. Currently, several papers on (Ba, Sr)-Si-O-N material systems with high quantum efficiency have been published, although the systems are not in use for commercial white LEDs mainly due to reliability issues. We believe that the reliability of the oxynitride phosphpor is related to this incomplete metamorphosis, which needs more study.

Achnowledgement

This research was supported by the Chung-Ang University Research Scholarship Grants in 2010 (Dong Wook Suh).

References

1. G. Blasse and A. Bril, J. Chem. Phys. 12 (1967) 5139.
2. J.K. Sheu, S.J. chang, C.H. Kuo, Y.K. Su, L.W. Wu, Y.C. Lin, W.C. Lai, J.M. Tsai, G.C. Chi, and R.K. Wu, IEEE Photon. Technol. Lett. 15 [1] (2003) 18-20.
3. J.K. Park, C.H. Kim, S.H. Park, H.D. Park and S.Y. Choi, Appl. Phys. Lett. 84 [10] (2004) 1647-1649.
4. N. Hirosaki, R.-J. Xie, K. Kimoto, T. Sekiguchi, Y. Yamamoto, T. Suehiro and M. Mitomo, Appl. Phys. Lett. 86 [21] (2005) 211905-3.
5. K. Sakuma, K. Omichi, N. Kimura, M. Ohashi, D. Tanaka, N. Hirosaki, Y. Yamamoto, R.-J Xie and T. Suehiro, Opt. Lett. 29 (2004) 2001-2003.
6. D.W. Suh, T.M. Lee, J.S. Yoo and S.H. Shin, J. Ceram. Proc. Res. 12 [S3] (2011) s289-s293.
7. W.H. Zhu, P.L. Wang, W.Y Sun and D.S. Yan, J. Mater. Sci. Lett. 13 [8] (1994) 560-562.
8. Y.Q. Li, A.C.A. Delsing, G. de With and H.T. Hintzen, Chem. Mater. 17 [12] (2005) 3242-3248.
9. O. Oeckler, F. Stadler, T. Rosenthal and W. Schnick, Solid State Sci. 9 [2] (2007) 205-212.
10. B.-G. Yun, Y. Miyamoto and H. Yamamoto, J. Electrochem. Soc. 154 [10] (2007) J320-J325.
11. T. Schlieper, W. Milius and W. Schnick, Z. Anorg. Allg. Chem. 621 [8] (1995) 1380-1384.
12. T. Schlieper and W. Schnick, Z. Anorg. Allg. Chem. 621 [6] (1995) 1037-1041.
13. Y.Q. Li, G. de With and H.T. Hintzen, J. Solid State Chem. 181[3] (2008) 515-524.
14. Y.Q. Li, J.E.J. van Steen, J.W.H. van Krevel, G. Botty, A.C.A. Delsing, F.J. DiSalvo, G. de With and H.T. Hintzen, J. Alloys. Compd. 417 [1-2] (2006) 273-279.
15. R.J. Xie, N. Hirosaki, T. Suehiro, F.F. Xu and M. Mitomo, Chem. Mater. 18 [23] (2006) 5578-5583.
16. G. Anoop, K.P. Kim, D.W. Suh, I.H. Cho and J.S. Yoo, Electrochem. Solid-State Lett. 14 [9] (2011) J58-J60.
17. X. Piao, T. Horikawa, H. Hanzawa and K. Machida, Appl. Phys. Lett. 88 [16] (2006) 161908-3.
18. J.A. Taylor, G.M. Lancaster, A. Ignatiev and J.W. Rabalais, J. Chem. Phys. 68 [4] (1978) 1776-1784.
19. R.P. Vasquez, J. Electron Spectrosc. Relat. Phemon. 56 [3] (1991) 217-240.
20. A. Ermolieff, P. Bernard, S. Marton, J.C. da Costa, J. Appl. Phys. 60 [9] (1986) 3162-3166.
21. Y.C. Fang, P.C. Kao, Y.C. Yang, S.Y. Chu, J. Electrochem. Soc. 158 [8] (2011) J246-J249.
22. D. Schalch, A. Scharmann and R. Wolfrat, Thin Solid Films 124 [3-4] (1985) 301-308.